

# A Decade's Progress in the Development of Molecular Imaging Agents Targeting the Growth Hormone Secretagogue Receptor

Marina D. Childs<sup>1</sup>  and Leonard G. Luyt<sup>1,2,3,4</sup> 

## Abstract

The growth hormone secretagogue receptor 1a (GHSR), also called the ghrelin receptor, is a G protein-coupled receptor known to play an important metabolic role in the regulation of various physiological processes, including energy expenditure, growth hormone secretion, and cell proliferation. This receptor has been implicated in numerous health issues including obesity, gastrointestinal disorders, type II diabetes, and regulation of body weight in patients with Prader-Willi syndrome, and there has been growing interest in studying its mechanism of behavior to unlock further applications of GHSR-targeted therapeutics. In addition, the GHSR is expressed in various types of cancer including prostate, breast, and testicular cancers, while aberrant expression has been reported in cardiac disease. Targeted molecular imaging of the GHSR could provide insights into its role in biological processes related to these disease states. Over the past decade, imaging probes targeting this receptor have been discovered for the imaging modalities PET, SPECT, and optical imaging. High-affinity analogues of ghrelin, the endogenous ligand for the GHSR, as well as small molecule inhibitors have been developed and evaluated both *in vitro* and in pre-clinical models. This review provides a comprehensive overview of the molecular imaging agents targeting the GHSR reported to the end of 2019.

## Keywords

advances in PET/SPECT probes, advances in optical probes, novel chemistry methods and approaches, medicinal chemistry, peptide chemistry, radiopharmaceutical

## Background

### *The GHSR and Its Endogenous Ligands*

The growth hormone secretagogue receptor (GHSR) is a member of the G protein-coupled receptor (GPCR) superfamily and was first identified in 1996 by Howard and co-workers.<sup>1</sup> It is also commonly referred to as the ghrelin receptor and exists in 2 known isoforms, GHSR-1a and GHSR-1b. The GHSR-1a is made up of 366 amino acids and is the only active form of the receptor. Isoform 1b is 289 amino acids in length with 100% sequence identity to that of the GHSR-1a up to Leu265. The GHSR-1a, hereafter referred to as GHSR, was first discovered in the pituitary and hypothalamus as a receptor that bound growth hormone secretagogues (GHS), a class of synthetic therapeutics developed to stimulate endogenous growth hormone secretion. Many GHS molecules were developed prior to the discovery and identification of the GHSR or its endogenous ligands; some of the many examples include GHRP-6, GHRP-2, hexarelin, MK 0677, G-7039, and ipamorelin.<sup>2-8</sup> Since that time, the GHSR has been found to be expressed in

tissues outside the CNS, including the pancreas, thyroid gland, spleen, adrenal gland, gastrointestinal tract, and cardiovascular system.<sup>9,10</sup> Intracellular signaling of this receptor is mediated by the endogenous ligand for the GHSR, ghrelin.

Kojima and coworkers first identified ghrelin in 1999 as the endogenous ligand for the GHSR ( $EC_{50} = 2.5$  nM).<sup>11</sup> Later, it was determined that the gene product is *preproghrelin*, which translates to a 117 amino acid polypeptide that is post-translationally cleaved after a 23 amino acid signal peptide to give the 94 amino

<sup>1</sup> Department of Chemistry, University of Western Ontario, London, Ontario, Canada

<sup>2</sup> Lawson Health Research Institute, London, Ontario, Canada

<sup>3</sup> Department of Oncology, University of Western Ontario, London, Ontario, Canada

<sup>4</sup> Department of Medical Imaging, University of Western Ontario, London, Ontario, Canada

### Corresponding Author:

Leonard G. Luyt, University of Western Ontario, 800 Commissioners Rd. E., London, Ontario, Canada N6A 4L6.

Email: lluyt@uwo.ca



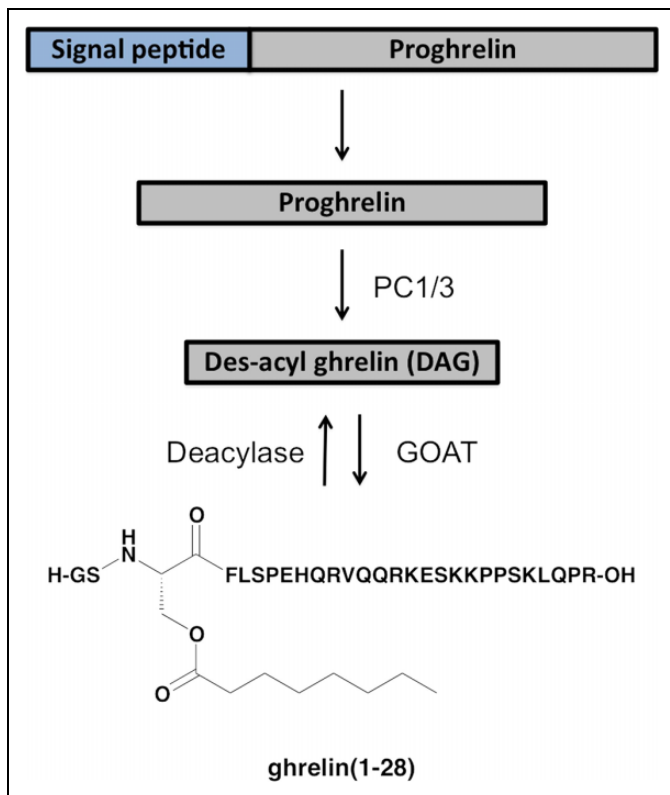


**Figure 1.** Biosynthetic processing from preproghrelin to ghrelin.

acid peptide, proghrelin (Figure 1).<sup>12</sup> Proghrelin may then be processed by prohormone convertase (PC) 1/3 to yield a 28 amino acid ghrelin peptide, and then acylated by ghrelin *O*-acyl transferase (GOAT) to produce bioactive ghrelin.<sup>13-15</sup> GOAT is a membrane-bound enzyme known to specifically attach an *n*-octanoyl fatty acid side chain off the serine residue in position 3 of ghrelin.<sup>13,14</sup> This unique acylation is essential in order for ghrelin to bind and activate the GHSR, whereas the non-acylated form of ghrelin, desacyl ghrelin (DAG), has no affinity for the receptor ( $IC_{50} > 10,000$  nM).<sup>16</sup> Interestingly, DAG is the predominant form of ghrelin found in circulation, but its particular function in relation to the receptor is still not fully understood. However, DAG does participate in physiological pathways independent of the GHSR including binding to the corticotropin releasing factor receptor type 2a (CRF2a), exerting beneficial actions on vascular function, and cardiac protection.<sup>17-19</sup> Additionally, a cyclic analogue of DAG, known as Livoletide, is currently in phase III clinical trials for the treatment of Prader-Willi syndrome.<sup>20</sup> The GHSR-1b isoform does not bind ghrelin or growth hormone secretagogues and, therefore, does not share the same signaling profile as the GHSR-1a.<sup>21</sup> The biological function of the GHSR-1b is still not well understood, though it has been shown to modulate the relatively high constitutive activity of the GHSR-1a through proposed hetero-dimerization of the 2 isoforms on the endoplasmic reticulum.<sup>22-24</sup> Therefore, the majority of the research on ligand development has been devoted exclusively to targeting the GHSR isoform 1a.



**Figure 2.** Amino acid sequence of mature LEAP2.

Recently in 2018, Ge et al. reported their discovery of liver-expressed antimicrobial peptide 2 (LEAP2) as a second endogenous ligand for the GHSR.<sup>25</sup> Mature LEAP2 is a 40 amino acid bicyclic peptide with 2 disulfide bridges, originally isolated in 2003 from human blood ultrafiltrate (Figure 2).<sup>26</sup> It was found to function as an antagonist for the receptor, causing inhibition of ghrelin-induced GHSR activation.<sup>25,27</sup> Later reports demonstrated that LEAP2 also behaved as an inverse agonist toward GHSR constitutive activity. M'Kadmi et al. found that LEAP2 displaces ghrelin from the orthosteric binding site of the GHSR ( $K_i = 1.26$  nM) and substantially decreased ghrelin-independent receptor signaling ( $EC_{50} = 22.8$  nM) in an inositol phosphate (IP1) production assay.<sup>28</sup> Similar to ghrelin, the full peptide sequence of LEAP2 is not necessary for the ligand to affect the receptor. Rather, the *N*-terminal region, LEAP2(1-14), which contains no disulfide bridges, is sufficient to maintain strong receptor binding ( $K_i = 3.66$  nM) and activity as an inverse agonist ( $EC_{50} = 76.4$  nM).<sup>28</sup> Furthermore, blocking endogenous LEAP2 was found to enhance ghrelin-induced GHSR activation *in vivo*.<sup>25</sup> The ability of LEAP2 to tune the ghrelin-GHSR system makes it an interesting therapeutic target for the treatment of metabolic diseases, such as obesity.

### Clinical Relevance of the GHSR Expression and Ghrelin Secretion

Activation of the GHSR by ghrelin results in a variety of physiological functions including regulation of appetite, energy homeostasis, growth hormone secretion, cell proliferation and survival, glucose and lipid metabolism, blood pressure regulation, and the protection of cells in the nervous and cardiovascular systems.<sup>29-33</sup> Research into perturbing the expression of ghrelin for the treatment of metabolic disorders, including anorexia, cachexia, obesity, and diabetes has resulted in the rapid expansion of reports of ghrelin receptor agonists, antagonists, and inverse agonists.<sup>34-37</sup> Several review articles exist summarize many of these ligands and their journey toward the clinic.<sup>8,38-40</sup> Additionally, altered GHSR and ghrelin expression has been observed in many cancers including pancreatic cancer, breast cancer, prostate cancer, ovarian cancer, gastric cancer, colon cancer, thyroid cancer, pituitary adenoma, and lung cancer.<sup>33,41-46</sup> Particularly, differential expression of the GHSR in prostate cancer tissues compared to benign hyperplasia was demonstrated by Lu et al, indicating a potential for use of the GHSR as a diagnostic biomarker for such cancers.<sup>47</sup> Therefore, targeted imaging of this receptor could provide a minimally invasive method for monitoring cancer treatment and progression. Moreover, the GHSR is abnormally expressed in cardiac pathology; increased expression has been demonstrated in the myocardium of patients with chronic heart failure

and decreased expression in patients with end-stage cardiomyopathy.<sup>41,48</sup> Related to these findings, ghrelin administration has been shown to have several therapeutic effects in cardiac disease including improving cardiac function in models of chronic heart failure.<sup>33</sup> As such, there is growing interest in developing ghrelin analogues for the purpose of imaging the biological processes related to cardiac GHSR. Current research to image the GHSR is underway through the development of probes derived from ghrelin, LEAP2, growth hormone secretagogues, and small molecules. While other reviews have provided overviews of ligands targeting a variety of GPCRs including the GHSR, this review seeks to provide a focused, stand-alone synopsis of molecular imaging agents targeting the GHSR reported to the end of 2019.<sup>49,50</sup>

## Review

### Molecular Imaging Agents Based on Ghrelin

Soon after the discovery of ghrelin, researchers were interested in elucidating the structure activity relationship (SAR) between this peptide hormone and its receptor. Early work focused on investigating the role of the aliphatic side-chain of ghrelin, the biological importance of the ester linkage to this side-chain, and the minimum sequence length required to maintain activation of the receptor.<sup>16,51</sup> These studies, reported in the early 2000s, determined that the octanoyl side-chain, while crucial for binding, could tolerate various structural modifications provided that sufficient hydrophobicity is retained. The ester group linking the aliphatic side-chain to the ghrelin peptide can be replaced by substituting serine-3 with diaminopropionic acid (Dpr), which affords a more chemically robust amide linkage with no detriment to the binding affinity. Furthermore, it was found that the *N*-terminal tetrapeptide, Gly-Ser-Ser(*n*-octanoyl)-Phe-NH<sub>2</sub>, was the smallest truncated analogue of ghrelin that could still activate the GHSR, albeit with low potency. Binding affinity and activation was stronger with longer analogues, such as ghrelin(1-10) and ghrelin(1-14). An alanine scan of ghrelin(1-14) systematically confirmed the importance of a positive charge at the *N*-terminus, identified Phe<sup>4</sup> as a critical residue for binding, and suggested that most other amino acids in the sequence could be replaced to further optimize affinity and potency.<sup>52</sup>

The last decade has seen a substantial increase in the number of imaging probes targeting the GHSR with 2009 marking the first publication investigating the potential to image this receptor as a cancer target. In this preliminary investigation, Rosita et al. reported on the development of ghrelin analogues bearing PET and SPECT imaging moieties.<sup>53</sup> The authors utilized structure-activity knowledge reported in the early years of ghrelin research to investigate 2 classes of ghrelin analogues. First, peptides containing fluorine within the aliphatic side chain of ghrelin were investigated as potential probes for <sup>18</sup>F-PET imaging. Peptides were synthesized and their binding affinities toward the GHSR were assessed via an *in vitro* radioligand-displacement binding assay. The resulting best candidate was a ghrelin(1-14) analogue bearing fluorine at the

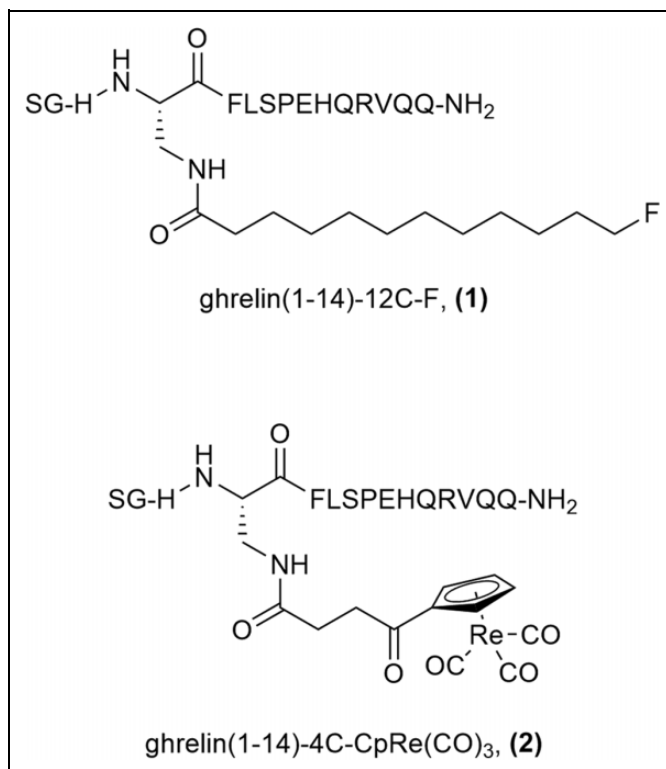


**Figure 3.** Fluorine and rhenium functionalized ghrelin analogues as potential GHSR-targeting PET and SPECT imaging probes.

end of a 12C side chain, ghrelin(1-14)-12C-F (**1**), which offered an IC<sub>50</sub> value of 27.9 nM.<sup>53</sup> The second class of ghrelin analogues investigated the potential to incorporate a <sup>185/187</sup>Re/<sup>99m</sup>Tc chelator into the aliphatic side chain for SPECT imaging. Most often, the imaging portion of a radiopharmaceutical is positioned far from the binding site so as not to have a negative affect on the binding affinity.<sup>54-58</sup> This is particularly common for radiotracers bearing metal chelators due to the relatively large size of the appended metal-complex. However, the authors chose to apply a more compact design that incorporates the imaging moiety in a position crucial for binding. Despite the added steric bulk, the relatively small and lipophilic organometallic species, cyclopentadienyl tricarbonyl (CpM(CO)<sub>3</sub>), was successfully incorporated into the side chain resulting in a Re-labeled ghrelin(1-14) analogue, ghrelin(1-14)-4C-CpRe(CO)<sub>3</sub> (**2**), with an IC<sub>50</sub> of 35 nM.<sup>53</sup> Peptides **1** and **2** (Figure 3) set the stage for future development of ghrelin-based GHSR imaging agents.

Later in 2015, Koźmiński and Gniazdowska continued work on developing SPECT imaging probes for the GHSR labeled with technetium-99 m (Figure 4).<sup>59</sup> The authors reported 3 analogues of ghrelin(1-7) conjugated to polydentate <sup>99m</sup>Tc-complexes via a bifunctional coupling agent (BFCA), isocyanobutyric acid succinimidyl ester, on a lysine residue at the *C*-terminus of the peptide. All analogues were produced in 85%-95% radiochemical yields and molar activities in the range of 20-25 GBq/μmol. First, a positively charged analogue, [Lys<sup>7</sup>(<sup>99m</sup>Tc(CO)<sub>3</sub>L<sub>N</sub>, <sup>o</sup>CN-BFCA)<sup>+</sup>]ghrelin(1-7) (**3**), was

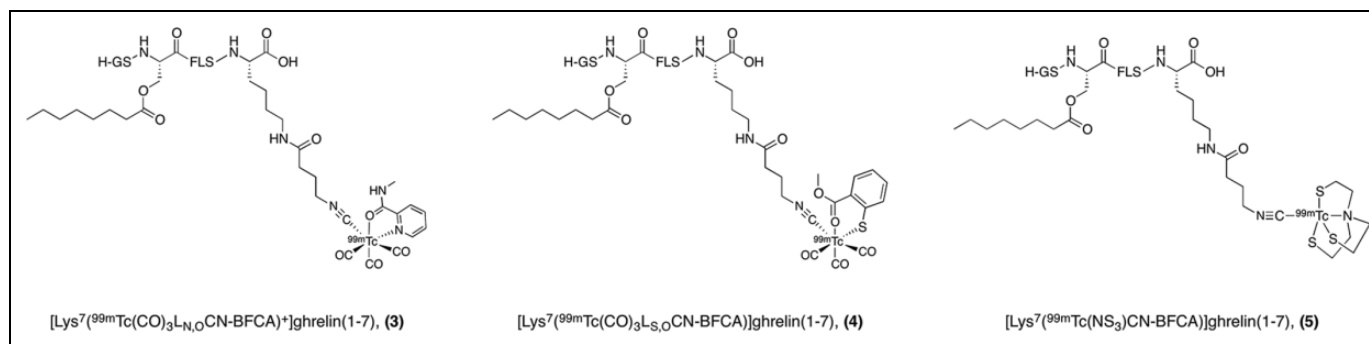


**Figure 4.**  $^{99m}Tc$ -SPECT imaging probes for the GHSR.

developed and labeled, but showed poor *in vitro* stability in human serum and was dismissed from further biological evaluation. A neutral analogue,  $[Lys^7(^{99m}Tc(CO)_3L_{S,O}CN-BFCA)]ghrelin(1-7)$  (**4**), which was stable in aqueous solutions and human serum, had a  $K_i$  value of 1.1 nM, but showed significant uptake in kidneys and liver (21% and 28% respectively at 30 min p.i.) when evaluated through an *in vivo* biodistribution study. In contrast, another stable but slightly more lipophilic analogue,  $[Lys^7(^{99m}Tc(NS_3)CN-BFCA)]ghrelin(1-7)$  (**5**), possessed a  $K_i$  value of 2.1 nM, and showed much lower kidney uptake but similar liver uptake compared to analogue **4** (2% and 29% at 30 min p.i.). These analogues represent the first  $^{99m}Tc$ -labeled ghrelin-based SPECT imaging agents.

During the early 2000s, the development of GHSR targeted probes was also underway outside the realm of nuclear imaging modalities. The first fluorescently labeled ghrelin analogue was reported by Enderle et al. with the goal of developing a non-radioactively labeled compound that could identify the GHSR and measure the binding affinity of other test compounds in cell-based assays.<sup>60</sup> The resulting analogues featured ghrelin truncated to the first 18 amino acids in the peptide sequence. A variety of maleimide-conjugated fluorophores, including Texas Red, tetramethyl rhodamine, BODIPY FL, and MR121, were conjugated to an additional cysteine residue on the C-terminus of the peptide to give analogues of the form:  $[Dpr(octanoyl)^3, Cys(dye)^{19}]ghrelin(1-19)$  amide.<sup>60</sup> In 2011, Leyris et al. developed a high-affinity red fluorescent ghrelin analogue, known as red-ghrelin, for use in a homogenous time-resolved fluorescence (HTRF) assay to screen ligands for the GHSR.<sup>61</sup> The biological properties of red-ghrelin were characterized and validated through a competitive radioligand displacement assay and inositol phosphate (IP1) accumulation. While the precise structure of this probe was not disclosed in the article, it was reported to bind to the GHSR with a  $K_i$  value of 19 nM and induce IP1 accumulation as efficiently as ghrelin with an  $EC_{50}$  value of 88 nM, approximately half as potent as their evaluation of native ghrelin. In addition to its use in the HTRF assay, red-ghrelin has also been used as a probe to localize GHSR expression and identify GPCR heteromerization in mouse brain.<sup>62,63</sup>

Later that year, McGirr et al. reported another fluorescently labeled ghrelin analogue for optical imaging of the GHSR (Figure 5).<sup>64</sup> The imaging label, fluorescein isothiocyanate (FITC), was incorporated onto the peptide via amide conjugation to the C-terminal lysine side chain, giving  $[Dpr(octanoyl)^3, Lys(flourescein)^{19}]ghrelin(1-19)$  (**6**). The  $IC_{50}$  value of this dye-labeled probe was 9.5 nM, which is comparable to hexarelin, a known GHSR agonist, and slightly weaker than natural ghrelin. Furthermore, this probe was used to provide the first visualization of GHSR *in situ* without the need for an antibody. GHSR expressing CHO cells were incubated with the probe and fluorescence imaging revealed distinct clustering of fluorescent signal indicative of receptor internalization. Additionally, specific binding was also observed in mouse cardiac tissue alluding to the interesting possibility of using ghrelin analogues for detecting GHSR expression in other tissues as well. Lu et al. further evaluated this probe as a tool in detecting the receptor in human prostate cancer vs. normal tissues.<sup>47</sup> The fluorescent signal from the probe bound to prostate cancer tissue was significantly higher when compared to normal tissue ( $P = 0.0093$ ) and benign hyperplasia ( $P = 0.0027$ ) following signal amplification, indicating differential receptor expression in these different tissues (Figure 6).

The success of the fluorescein ghrelin probe in GHSR detection prompted its use in other biological studies. Indeed, since its development, this probe has been used on numerous occasions in the identification of ghrelin binding sites in genetically engineered cells and in mouse brain tissue.<sup>65-68</sup> The brain areas accessible to ghrelin have been elucidated by systematically mapping the distribution of centrally or peripherally administered tracer **6** in the mouse brain, demonstrating uptake in GHSR expressing brain areas.<sup>69-72</sup> Further efforts utilized this probe to better illuminate the possible mechanisms by which circulating ghrelin accesses its receptor in the brain.<sup>70,73,74</sup> Other studies have used probe **6** to investigate the ability for ghrelin to interact with plasma proteins such as serum albumin, and the ability for GHSR to interact with other GPCRs.<sup>75,76</sup>

However, due to interference by tissue autofluorescence and the dye's susceptibility to photobleaching, the fluorescein dye was replaced with a more stable, far-red sulfonated cyanine 5 dye

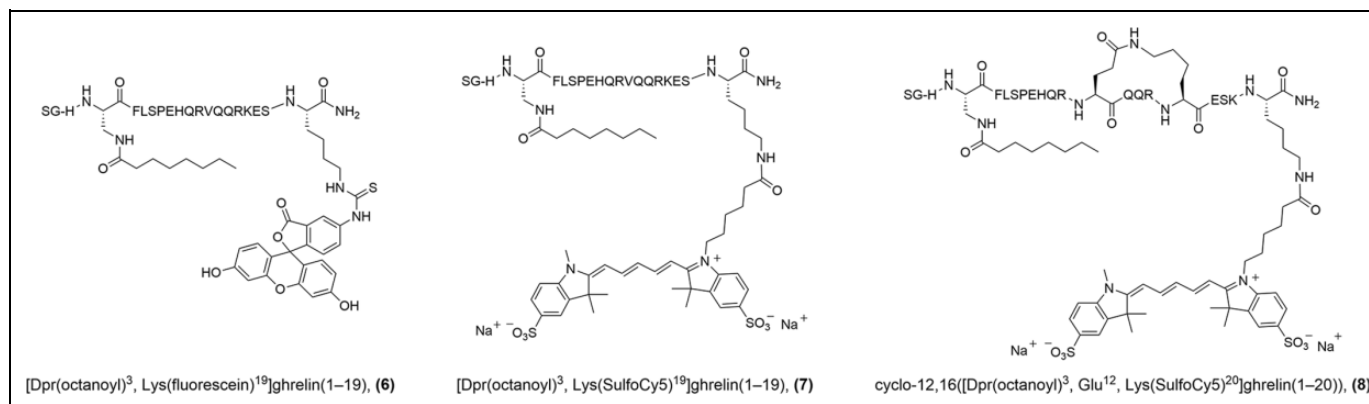


**Figure 5.** Ghrelin-derived fluorescent probes for optical imaging of the GHSR.

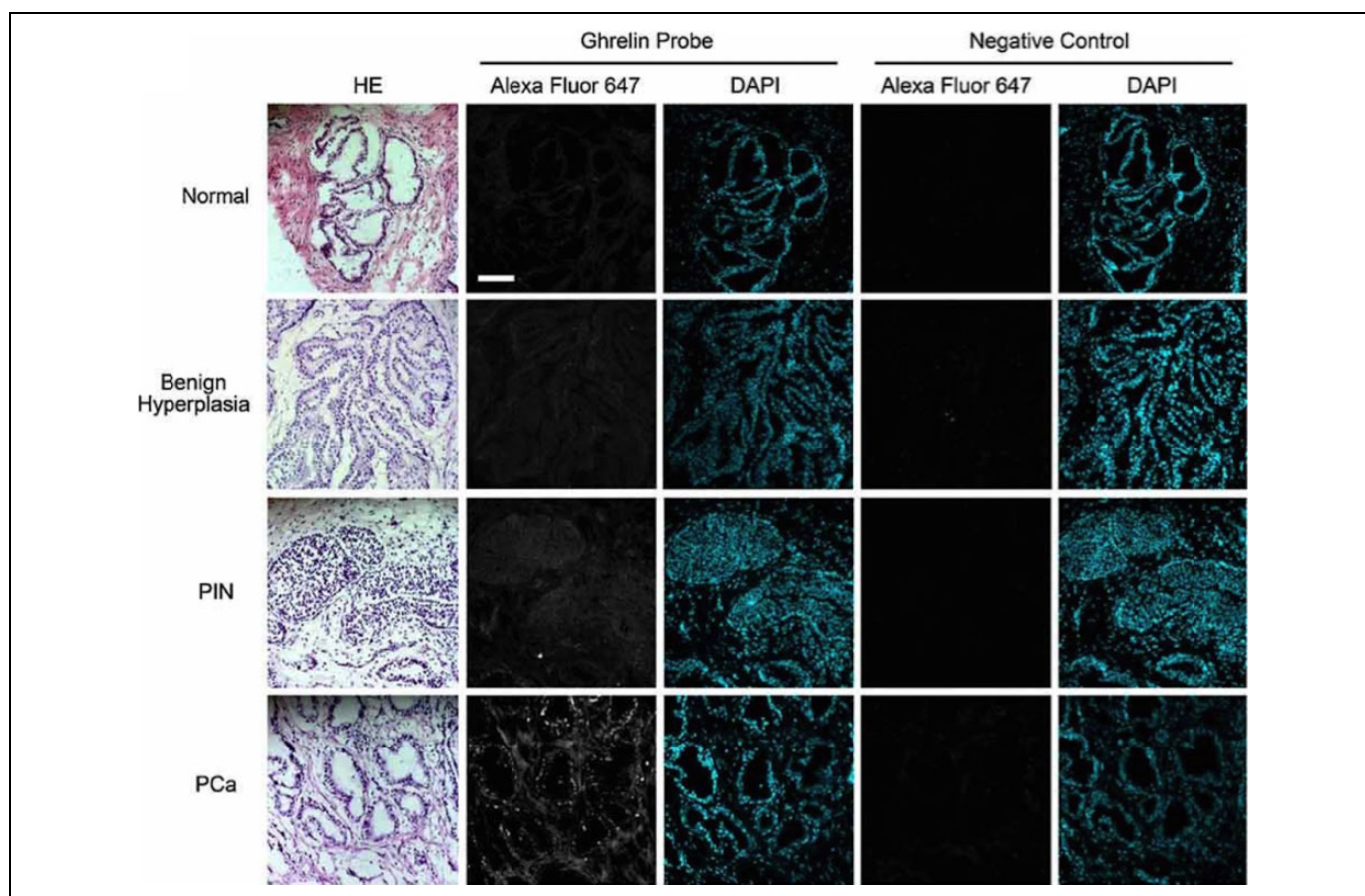


**Figure 6.** Differential ghrelin probe binding in prostate cancer *ex vivo*. Ghrelin probe binding was evaluated in benign tissue subdivided into normal and hyperplasia, prostatic intraepithelial neoplasia (PIN), and prostate cancer using the hapten amplification approach. Negative control was processed in the absence of ghrelin probe. Grayscale = ghrelin probe, Blue = DAPI. Scale bar = 10  $\mu\text{m}$ .<sup>47</sup> Reprinted with permission from John Wiley and Sons.

(SulfoCy5) producing the ghrelin-based probe, [Dpr(octanoyl)<sup>3</sup>, Lys(SulfoCy5)<sup>19</sup>]ghrelin(1–19) (7). Douglas et al. reported on the new probe (Figure 5), which was determined to have an IC<sub>50</sub> value of 25.8 nM, a decrease in GHSR affinity compared to the fluorescein-containing peptide.<sup>77</sup> Nevertheless, the SulfoCy5-labeled ghrelin analogue was not only able to detect cardiac

GHSR expression, but it was also able to track GHSR expression during differentiation of P19-derived cardiomyocytes. Since then, this analogue has been used to detect the dynamics of myocardial GHSR in a mouse model of diabetic cardiomyopathy and before and after cardiac transplantation in humans, indicating the utility of fluorescent peptide analogs in mapping

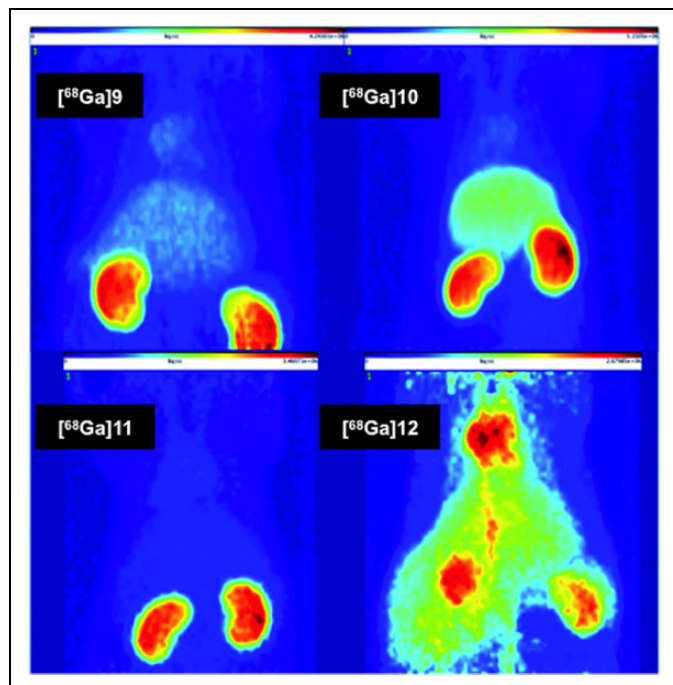


**Figure 7.** Maximum intensity projection of PET studies of  $^{68}\text{Ga}$ -labeled compounds  $[^{68}\text{Ga}]9-12$  at 5 min midframe time (duration of measurement: 6 min). The images were scaled to the maximum activity ( $\text{Bq}\cdot\text{cm}^{-3}$ ) in each image.<sup>57</sup> Adapted with permission from ref. 57. Copyright 2012 American Chemical Society.

GHSR expression in healthy, developing, and diseased heart models, as well as human hearts.<sup>78,79</sup>

The increasing promise of fluorescently labeled ghrelin analogues contributed to a desire to develop ghrelin imaging probes with improved metabolic stability. Recently, ghrelin(1-20) was cyclized through a lactam bridge between Glu<sup>12</sup> and Lys<sup>16</sup> for improved stability of secondary structure, and labeled with the SulfoCy5 dye off the C-terminal lysine residue (Figure 5).<sup>80</sup> This stapled peptide, cyclo-12, 16[Dpr(octanoyl)<sup>3</sup>, Glu<sup>12</sup>, Lys(SulfoCy5)<sup>20</sup>]ghrelin(1-20) (**8**), was reported to have an  $\text{IC}_{50}$  value of 1.0 nM, which is an improved affinity compared to any previously reported fluorescent ghrelin analogue, and was found to image receptor expression in 3 ovarian cancer cell lines: OvCar8 GHSR positive cells as well as parental OvCar3 and HEYA8 cells.

The ability to incorporate a bulky dye off the C-terminus of truncated ghrelin opened up the possibility of implementing other imaging moieties such as radionuclide-containing prosthetic groups or radiometal chelators in that position, while maintaining desirable binding affinities in the low nanomolar range. Chollet et al. developed full length ghrelin(1-28) and truncated ghrelin(1-16) agonists labeled with gallium-68 via a 7-triazacyclononane,1-glutaric acid-4,7-acetic acid (NODAGA) chelator for PET imaging (Figure 8).<sup>57</sup> Highly potent [Ga]-NODAGA peptide conjugates were synthesized and their ligand-receptor interactions were characterized through an inositol triphosphate (IP3) turnover assay resulting

in  $\text{EC}_{50}$  values in the 0.7-2.0 nM range. Initially, the chelator was conjugated to the peptide at the N-terminus, and, unsurprisingly, the modification was not well tolerated and  $N^{\alpha}$ -NODAGA(Ga)-ghrelin(1-28) lost all activity toward the receptor. It is well established in the literature that an available N-terminus is necessary for ligand-receptor binding between ghrelin and the GHSR.<sup>16,51</sup> Conversely, by placing the chelator on the Lys<sup>16</sup> residue, away from the N-terminal region of the peptide (**9**, **10**, **11**), the agonistic activity was restored. Analogues **9** and **10** contained the full ghrelin(1-28) sequence while analogue **11** was truncated to the first 16 amino acids. No significant difference in  $\text{EC}_{50}$  value arose due to the length of the peptide. The possibility of using such radiotracers to study ghrelin signaling *in vivo* also prompted the authors to develop an inverse agonist probe in parallel with the agonist probes.  $N^{\alpha}$ -NODAGA(Ga)-KwFwLL-CONH<sub>2</sub> (**12**) is based off a hexapeptide inverse agonist for the GHSR previously developed by the same group.<sup>81</sup> Similar to  $N^{\alpha}$ -NODAGA(Ga)-ghrelin(1-28), the inverse agonist conjugate contained the chelator on the N-terminus resulting in a substantial, but not complete, loss in inverse agonist activity toward the receptor. All 3  $^{68}\text{Ga}$ -labeled agonists and the radiolabeled inverse agonist were evaluated *in vivo* to analyze their pharmacokinetic and non-specific biodistribution profiles. The agonists showed fast blood clearance, poor *in vivo* stability, and high kidney accumulation (Figure 7). In contrast, the inverse agonist was found to have slower blood clearance, higher stability, wider tissue distribution, and favored hepatobiliary metabolism (Figure 7). Likely, the peptidomimetic nature of  $[^{68}\text{Ga}]12$  protects it from metabolic degradation, whereas the natural ghrelin sequence is easily recognizable by peptidases.

Another example of incorporating imaging moieties off the C-terminus of ghrelin was reported by Murrell et al.<sup>82</sup> The authors developed a novel  $^{18}\text{F}$ -prosthetic group based on an azadibenzocyclooctyne (ADIBO) scaffold and demonstrated its ability to be incorporated into biomolecules through successful conjugation to ghrelin(1-19) with minimal effects on the binding affinity (Figure 9). The resulting peptide analogue, [Dpr<sup>3</sup>(octanoyl), Lys<sup>19</sup>(triazole-ADIBO-F)]ghrelin(1-19) (**13**), was found to have an  $\text{IC}_{50}$  value of 9.7 nM and was labeled with fluoride-18 to produce  $[^{18}\text{F}]13$  in radiochemical yields of 64-66% and molar activities of 0.6-0.9 GBq/ $\mu\text{mol}$ .<sup>82</sup>

Charron et al. continued with this theme and reported a probe containing a 1,4,7,10-tetraazacyclododecane-1,4,7,10-tetraacetic acid (DOTA) chelator off the C-terminal lysine residue (Figure 8), [Dpr<sup>3</sup>(octanoyl), Lys<sup>19</sup>(Ga-DOTA)]ghrelin(1-19) (**14**), which possessed an  $\text{IC}_{50}$  value of 5.9 nM, comparable to natural ghrelin ( $\text{IC}_{50} = 3.1$  nM).<sup>58</sup> The probe was labeled with gallium-68 in radiochemical yields of 54%-83% and molar activities of 10.2-22.8 GBq/ $\mu\text{mol}$ . Pre-clinical PET imaging was done on NOD-SCID male mice using 2 cancer cell lines for xenograft studies: HT1080/GHSR and parental HT1080 cells. While  $[^{68}\text{Ga}]14$  did show increased uptake in the HT1080/GHSR xenografts compared to the parental HT1080 xenograft, significant accumulation in the kidneys prompted the authors to not pursue further *in vivo* evaluation,

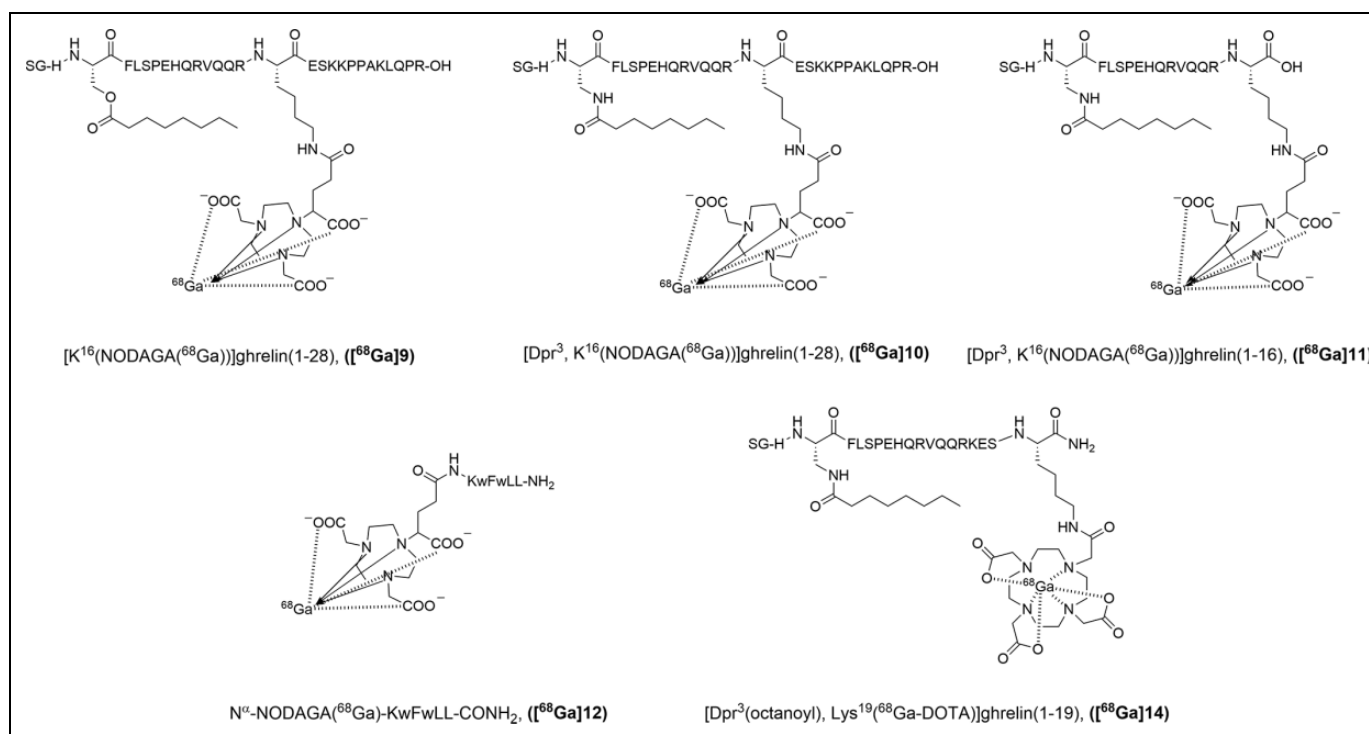


**Figure 8.** Gallium-68 labeled imaging probes for PET imaging of the GHSR.

but rather to focus their efforts on developing shorter ghrelin analogues with improved pharmacokinetic profiles.

Indeed, the same group conducted an extensive structure-activity relationship campaign to develop a truncated ghrelin(1-8) analogue that maintained high affinity for the GHSR.<sup>83</sup> This SAR investigation on the *N*-terminal ghrelin(1-8) sequence identified favorable modifications to residues 1, 3, 4, and 8 resulting in the peptide analogue,  $[\text{Inp}^1, \text{Dpr}^3(6\text{-fluoro-2-naphthoate}), 1\text{-Nal}^4, \text{Thr}^8]\text{ghrelin}(1-8)$  amide (**15**), which possessed an unprecedented  $\text{IC}_{50}$  value of 0.11 nM, the strongest affinity ghrelin analogue reported to date (Figure 9).<sup>83</sup> Undoubtedly, the most intriguing modification in this analogue is the substitution of the *n*-octanoyl side chain on residue 3 for a fluorine-containing aromatic moiety. Interestingly, this is not the only instance where aromatic substituents were incorporated onto residue 3 of a ghrelin analogue. In 2015, Zhao et al. reported a new class of GOAT inhibitors containing aromatic groups conjugated to the ghrelin sequence in this position via a triazole linkage.<sup>84</sup> However, the residue 3 aromatic moiety in peptide **15** not only contributed to the favorable binding affinity of the compound, but also added a fluorine atom for  $^{18}\text{F}$ -labeling. A molecular docking study using a homology model of the GHSR suggested the naphthyl group not only occupied a hydrophobic subpocket of the receptor's orthosteric site, but also proposed an H-bond interaction between the fluorine atom and Val 205 thereby enhancing the binding affinity.<sup>83,85</sup> To label this compound with fluoride-18, a novel  $[\text{18F}]6\text{-fluoro-2-pentafluorophenyl naphthoate}$  ( $[\text{18F}]\text{PFPN}$ ) prosthetic group was synthesized via nucleophilic

aromatic substitution with fluoride-18, but resulted in low radiochemical yields of the radiofluorinated product  $[\text{18F}]\text{15}$  (3.1% RCY), which presents a challenge for *in vivo* evaluation. Likely, the aromatic naphthyl moiety was not sufficiently activated to facilitate the necessary substitution reaction.

### Molecular Imaging Agents Based on Other Peptides and Peptidomimetics

Until 2018, most reported peptidic GHSR targeted imaging probes were derived from endogenous ghrelin (Table 1). Fowkes et al. sought to develop a growth hormone secretagogue-based probe for PET imaging of the GHSR.<sup>86</sup> The authors studied an extensive number of growth hormone secretagogues including GHRP-1, GHRP-2, GHRP-6, ipamorelin, and G-7039 as potential  $^{18}\text{F}$ -PET imaging agents. The fluorine-modified secretagogue derivative with the strongest binding affinity for the GHSR was  $[\text{1-Nal}^4, \text{Lys}^5(4\text{-fluorobenzoate})]\text{G-7039}$  (**16**) (Figure 9), with an  $\text{IC}_{50}$  value of 69 nM and an  $\text{EC}_{50}$  value of 1.1 nM based on  $\text{Ca}^{2+}$ -mobilization. Conjugation of a *N*-succinimidyl-4- $[\text{18F}]\text{fluorobenzoate}$  ( $[\text{18F}]\text{SFB}$ ) prosthetic group to  $[\text{1-Nal}^4]\text{G7039}$  afforded  $[\text{18F}]\text{16}$  in an average, overall radiochemical yield of 48% ( $n = 3$ ) and molar activity  $>34$  GBq/ $\mu\text{mol}$ . This probe was further analyzed through *in vivo* PET imaging of cardiac GHSR.<sup>87</sup> *Ex vivo* biodistribution revealed that tracer distribution was independent of circulating levels of endogenous ghrelin. However, no significant correlation between tracer uptake and GHSR expression in the heart was observed and there was significant uptake in off

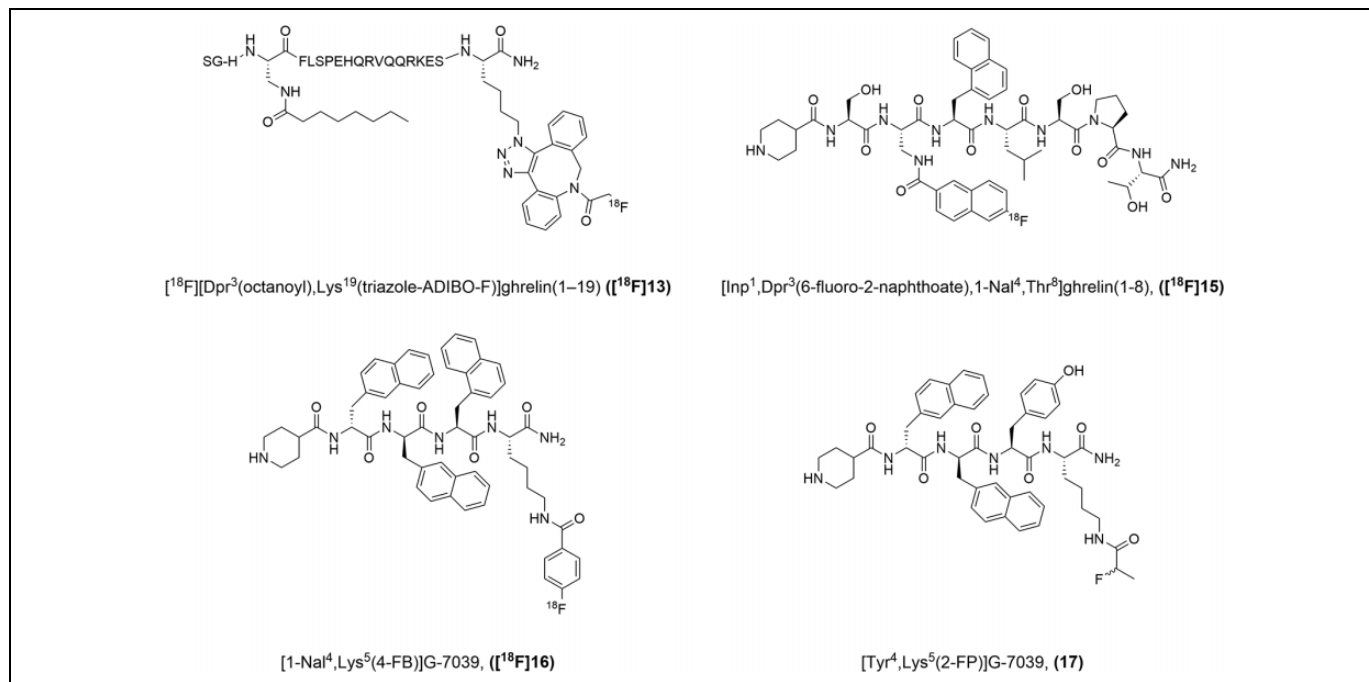


**Figure 9.** Peptidic and peptidomimetic probes for fluorine-18 PET imaging of the GHSR.

target tissues, such as the liver, spleen, lungs, and kidneys. Some of the issues that may have led to the tracer's poor performance *in vivo* include the relatively weak binding affinity for a PET imaging agent and the high cLogP value of 8.76. To address these challenges, Lalonde et al. replaced the 4-fluorobenzoyl prosthetic group off the Lys<sup>5</sup> side chain with a 2-fluoropropionyl (2-FP) group and performed a focused SAR study at the fourth position of ligand **16**.<sup>88</sup> A single amino acid replacement of 1-Nal<sup>4</sup> with tyrosine was identified producing a new ligand for the GHSR, [Tyr<sup>4</sup>, Lys<sup>5</sup>(2-FP)]G-7039 (**17**) with improved properties (Figure 9). Compound **17** was determined to have a 70-fold increase in binding toward the receptor ( $\text{IC}_{50} = 0.28$  nM) and a significantly lower cLogP value of 2.77. However, radiosynthesis and *in vivo* evaluation of this new ligand has yet to be reported.

The recent identification of LEAP2 as a second endogenous ligand for the GHSR prompted a desire to develop a fluorescent analogue of LEAP2 suitable for studying the pharmacological behavior of GHSR: LEAP2 complexes compared to those of GHSR: ghrelin.<sup>25,27,28</sup> Barrile et al. recently reported the resulting fluorescent ligand, LEAP2(1-17)-DY-647P1 (**18**), also referred to as F-LEAP2, which is based on the first 17 amino acids of the mature peptide sequence (Figure 10).<sup>89</sup> By taking advantage of Cys<sup>17</sup>, which traditionally forms an intramolecular disulfide bridge with Cys<sup>28</sup> in the endogenous sequence, the authors were able to conjugate a DY-647P1 fluorophore to the C-terminus of the ligand. Compound **18** was confirmed to bind strongly to the GHSR with a  $K_i$  value of 3.9 nM, which is similar to that of native LEAP2 ( $K_i = 1.26$  nM) and LEAP2(1-14) ( $K_i = 3.66$  nM).<sup>28</sup> Furthermore, analogue **18** caused a decrease in constitutive

GHSR activity in a GPT $\gamma$ S functional assay, indicating that the inverse agonist properties of the peptide were not affected by the addition of the fluorophore. An *in vivo* bioactivity assessment study revealed that pre-treatment of mice with ICV-injected **18** inhibited ghrelin-induced food intake by ~40%, similar to native LEAP2. Additionally, cell imaging studies of the new probe showed that the fluorescent signal was limited to the cell surface indicating that the fluorescently-labeled peptide does not induce receptor internalization, which is consistent with previous reports.<sup>27</sup> Finally, *ex vivo* imaging of mouse brain tissue indicated the strongest intensity of **18** was located in the hypothalamus, consistent with the high receptor expression reported for this brain region. LEAP2(1-17)-DY-647P1 represents the first probe based on an antagonist/inverse agonist for fluorescence imaging of the GHSR and could be a valuable tool for further pharmacological analyses of this receptor.

### Molecular Imaging Agents Based on Small Molecules

In 2007, Bayer pharmaceuticals reported a number of quinazolinone derivatives as a new class of small molecule GHSR antagonists for the treatment of obesity and diabetes.<sup>90</sup> The piperidine-substituted quinazolinone scaffold (Figure 11) showed inherently nanomolar affinity for the receptor, while alkylating the piperidine ring nitrogen ( $R_1$ ) gave rise to the functionally antagonistic activity.

In 2011, Potter et al. sought to utilize this class of high-affinity small molecules to develop GHSR targeting PET radioligands.<sup>91</sup> One of the molecules reported by Bayer, racemic 6-(4-fluorophenoxy)-3-(piperidin-3-yl)methyl)-2-*o*-tolylquinazolin-4(3H)-one (**19**), possessed a binding affinity

of  $K_i = 0.9$  nM toward the GHSR (Figure 12).<sup>90</sup> The authors modified this compound to incorporate a carbon-11 radionuclide off the piperidine nitrogen ( $R_1$ ). The resulting imaging probe, (**20**), was synthesized and found to bind to the GHSR with a  $K_i$  value of 22 nM (Figure 12). Compound [<sup>11</sup>C]**20** was labeled in a non decay-corrected radiochemical yield of 25%, a molar activity of 8300 mCi/ $\mu$ mol, and a radiochemical purity of 99%. Due to the high density of the receptor in the

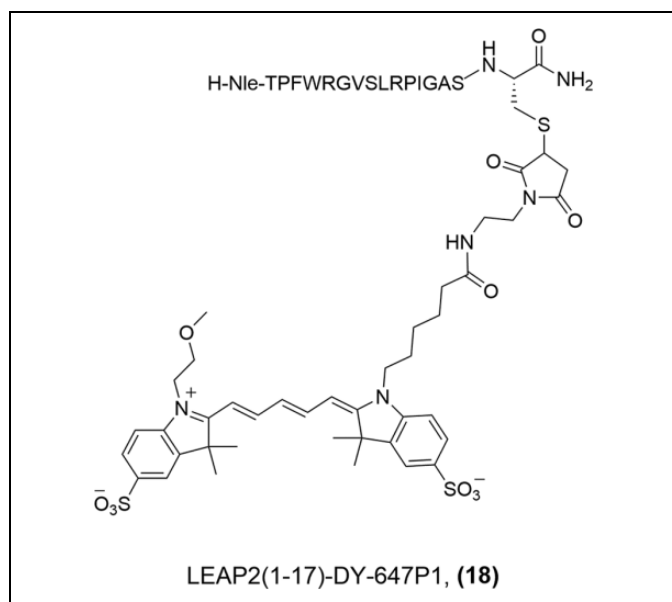


**Figure 10.** Fluorescently labeled LEAP-2 derivative for optical imaging of the GHSR.

hypothalamus and pituitary, the authors sought to evaluate their probe as a potential radiotracer for brain PET imaging of the GHSR. *In vivo* PET imaging in mice revealed low tracer accumulation in the hypothalamus with a gradual increase in uptake to 0.86% ID/g over the 90 minute imaging period. Signal in the hypothalamus was significantly blocked with **19**, indicating receptor-mediated uptake. However, some tracer uptake in the rest of the brain, made up of tissues with low GHSR density, indicated non-specific tracer uptake, which was confirmed in a blocking study. The authors postulated that the lipophilicity of the tracer ( $\text{clogD} = 4.1$ ) may be too high to be an effective CNS radioligand and recommended that future GHSR radioligands for brain PET imaging have picomolar binding affinities and lower lipophilicities. Of note, this was the first report of a radiolabeled imaging probe for PET imaging of the GHSR and the first report of *in vivo* GHSR imaging data.

Later in 2017, Kawamura et al. continued the endeavor of labeling small molecule GHSR antagonists with PET radionuclides and reported 3 new radioligands: **21**, **22**, and **23** (Figure 13)

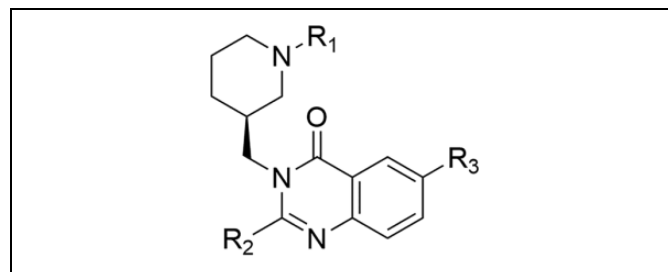


**Figure 11.** General scaffold for quinazolinone-derived small molecule GHSR imaging probes.

**Table 1.** *In vitro* Properties and Radiosynthetic Results of Peptidic GHSR Imaging Probes.

Compound No.	IC <sub>50</sub>	EC <sub>50</sub>	RCY	clogD	Imaging Modality	Ref.
<b>1</b> (fig. 3)	27.9 nM	N.R.	N.R.	N.R.	<sup>18</sup> F-PET	53
<b>2</b> (fig. 3)	35 nM	N.R.	N.R.	N.R.	<sup>99m</sup> Tc-SPECT	53
<b>3</b> (fig. 4)	N.R.	N.R.	> 85%	0.73 <sup>[b]</sup>	<sup>99m</sup> Tc-SPECT	59
<b>4</b> (fig. 4)	1.1 nM <sup>[a]</sup>	N.R.	> 85%	0.88 <sup>[b]</sup>	<sup>99m</sup> Tc-SPECT	59
<b>5</b> (fig. 4)	2.1 nM <sup>[a]</sup>	N.R.	> 95%	1.10 <sup>[b]</sup>	<sup>99m</sup> Tc-SPECT	59
red-ghrelin	19 nM <sup>[a]</sup>	88 nM	N/A	N.R.	Optical	61
<b>6</b> (fig. 5)	9.5 nM	N.R.	N/A	N.R.	Optical	64
<b>7</b> (fig. 5)	25.8 nM	N.R.	N/A	N.R.	Optical	77
<b>8</b> (fig. 5)	1.0 nM	N.R.	N/A	N.R.	Optical	80
<b>9</b> (fig. 8)	N.R.	0.72 nM	N.R.	N.R.	<sup>68</sup> Ga-PET	57
<b>10</b> (fig. 8)	N.R.	1.91 nM	N.R.	N.R.	<sup>68</sup> Ga-PET	57
<b>11</b> (fig. 8)	N.R.	1.41 nM	N.R.	N.R.	<sup>68</sup> Ga-PET	57
<b>12</b> (fig. 8)	N.R.	643.2 nM	N.R.	N.R.	<sup>68</sup> Ga-PET	57
<b>13</b> (fig. 9)	9.7 nM	N.R.	64-66%	N.R.	<sup>18</sup> F-PET	82
<b>14</b> (fig. 8)	5.9 nM	N.R.	54-83%	N.R.	<sup>68</sup> Ga-PET	58
<b>15</b> (fig. 9)	0.11 nM	N.R.	3.1%	N.R.	<sup>18</sup> F-PET	83
<b>16</b> (fig. 9)	69 nM	1.1 nM	48%	8.76	<sup>18</sup> F-PET	86
<b>17</b> (fig. 9)	0.28 nM	0.121 nM	N.R.	2.77	<sup>18</sup> F-PET	88
<b>18</b> (fig. 10)	3.9 nM <sup>[a]</sup>	N.R.	N.R.	N.R.	Optical	89

N.R. – not reported.

<sup>[a]</sup> Reported as  $K_i$ .

<sup>[b]</sup> Lipophilicity determined experimentally.

with low nanomolar binding affinities ( $K_i = 16$  nM, 4.0 nM, 7.0 nM respectively).<sup>92</sup> Compound **21** was labeled with fluoride-18 in a low radiochemical yield of 2.5% and a high molar activity of 300 GBq/ $\mu$ mol. Compounds **22** and **23** were labeled with carbon-11 in radiochemical yields of 1.7% and 16%, respectively and molar activities of 240 GBq/ $\mu$ mol and 100 GBq/ $\mu$ mol, respectively. *In vivo* biodistribution studies showed relatively low levels of tracer uptake in the mouse brain for all 3 radioligands, likely due to their relatively high lipophilicities (Table 2). Compound [<sup>18</sup>F]**21** exhibited increased bone uptake over 60 min post-injection (p.i.), indicative of <sup>18</sup>F-defluorination. Interestingly, compound [<sup>11</sup>C]**23** exhibited relatively high tracer uptake in the pancreas (6.5% ID/g) at 60 min p.i. Pre-treatment of the mouse with 10 mg/kg of a high-affinity GHSR antagonist, YIL781 ( $K_i = 17$  nM),<sup>93</sup> resulted in significantly less uptake of [<sup>11</sup>C]**23** in the pancreas at 60 min p.i. However, this change in radioactive signal was found to be dependent on the tracer administered. Compound [<sup>11</sup>C]**23** showed the largest decrease in signal (20%) with pre-treatment of YIL781 compared to [<sup>11</sup>C]**22** and [<sup>18</sup>F]**21**, which showed little to no change in signal compared to the control. Figure 14 shows a representative PET image of [<sup>11</sup>C]**23** uptake with and without pre-treatment with the antagonist.

Another group seeking to generate compounds suitable for GHSR imaging in the brain reported a SAR study on fluorinated quinazolinone derivatives with low nanomolar affinities.<sup>94</sup>

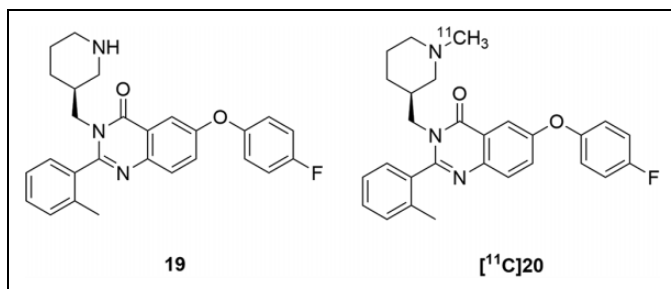


**Figure 12.** Quinazolinone derivative reported by Bayer pharmaceuticals (**19**) and resulting <sup>11</sup>C-labeled probe ([<sup>11</sup>C]**20**) from Potter et al.<sup>91</sup>

Substitution at the piperidine nitrogen is known to have an effect on binding to the receptor; therefore, the authors chose a known, high affinity, quinazolinone derivative as a starting point for SAR studies, compound **24**.<sup>95</sup> Results from the study revealed that both enantiomers of the original lead candidate, (*S*)-**24** and (*R*)-**24**, and a new derivative, (*S*)-**25** had the strongest binding affinities ( $IC_{50} = 2.2$  nM, 3.9 nM, and 2.7 nM, respectively). Further *in vitro* evaluation of (*S*)-**24**, (*R*)-**24**, (*S*)-**25** confirmed all 3 molecules to be potent partial agonists with  $EC_{50}$  values of 0.7 nM, 0.6 nM, and 1.0 nM, respectively (Figure 15). Furthermore, the calculated  $\log D_{7,4}$  values for these compounds were lower than previously reported quinazolinone derivatives ( $\text{clog}D_{7,4} = 2.1$  for (*R/S*)-**24** and  $\text{clog}D_{7,4} = 2.9$  for (*S*)-**25**), which are expected to be favorable for brain imaging. However, the difficulty with these compounds lies in their ability to be translated into radiolabeled imaging agents. While each molecule possesses a fluorine atom, the position of the aromatic fluorine is challenging for <sup>18</sup>F-labeling due to the weakly activated nature of the aromatic ring for conventional substitution techniques. The use of relatively mild <sup>18</sup>F-fluorination methodologies for such difficult aromatic molecules is becoming more commonplace; however, radiolabeling of these molecules has yet to be reported.

The most recent attempt to develop quinazolinone derivatives for <sup>18</sup>F-fluorine PET imaging of the GHSR was reported in 2018 by Hou et al.<sup>96</sup> The authors also used the compound

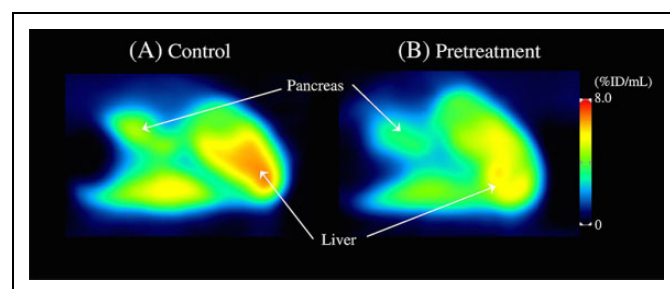


**Figure 14.** Representative PET images of mice using [<sup>11</sup>C]**23** (20-50 MBq/140-520 pmol) in the control (A) and pretreatment with YIL781 (10 mg/kg b.w.) conditions.<sup>92</sup> Reprinted with permission from Elsevier.

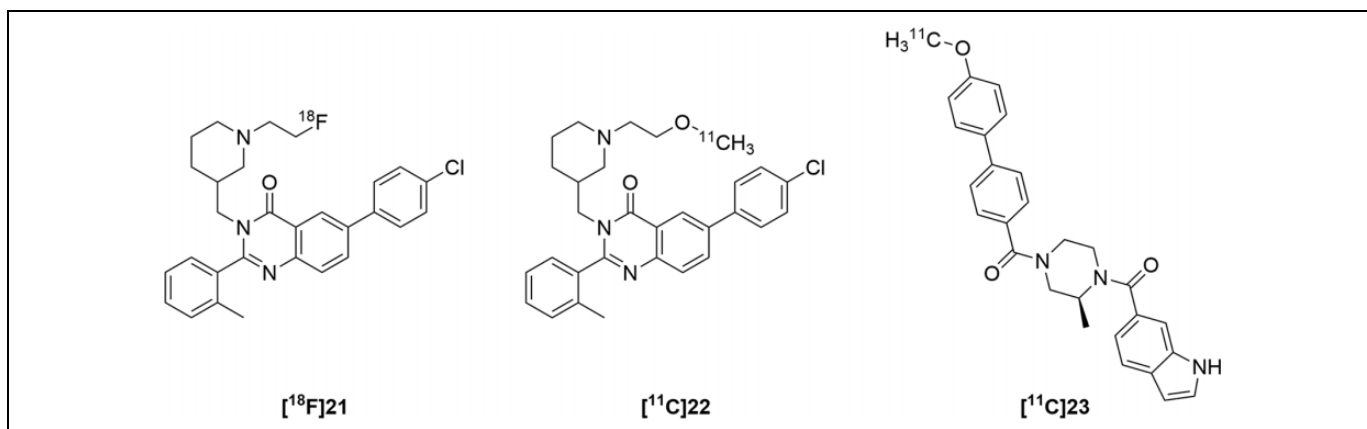


**Figure 13.** Structures of small molecule GHSR antagonists for <sup>18</sup>F-PET and <sup>11</sup>C-PET imaging reported by Kawamura et al.<sup>92</sup>

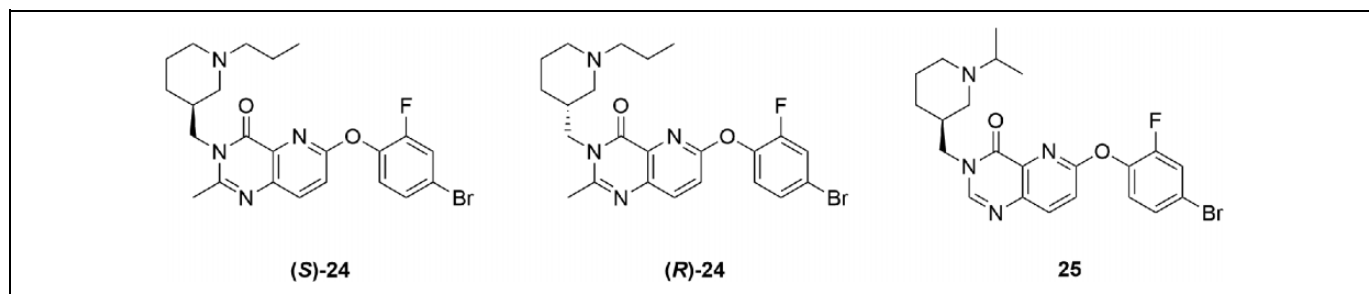


**Figure 15.** High affinity quinazolinone-derived partial agonists for the GHSR reported by Moldovan et al.<sup>94</sup>

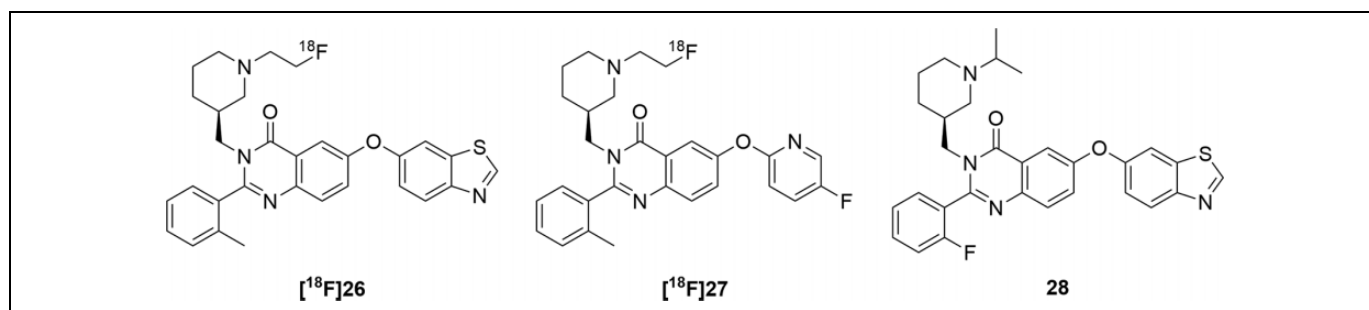


**Figure 16.** Small molecule quinazolinone analogues reported by Hou et al for  $^{18}\text{F}$ -PET imaging of the GHSR.<sup>96</sup>

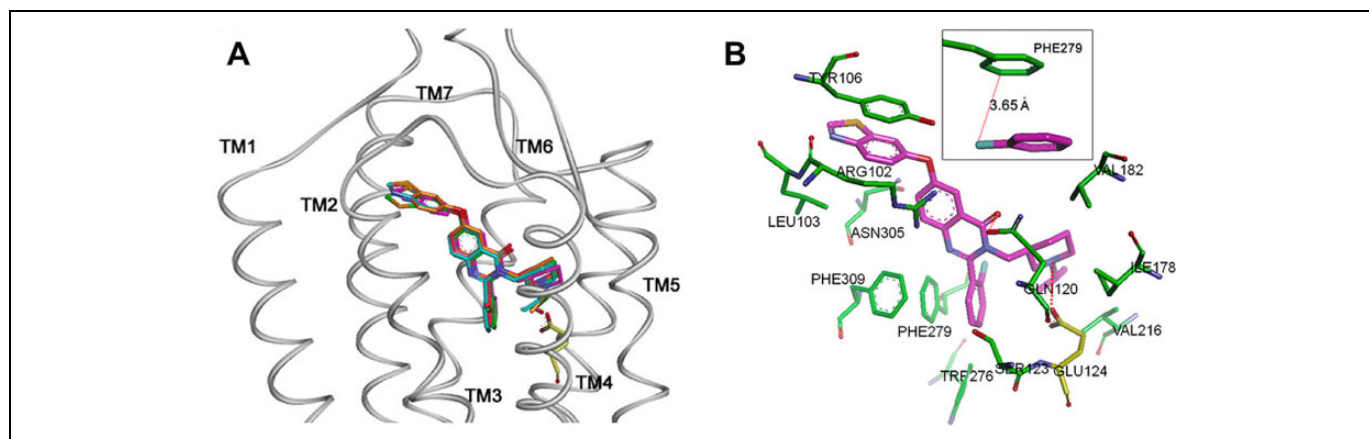


**Figure 17.** The complex structures from molecular docking studies using a homology model of GHS-R1a. (A) Side view of quinazolinone derivatives superimposed in the GHS-R1a; (B) A view from extracellular side; 3D depiction of the binding mode and surrounding residues for compound **28**. Ligands are shown in purple sticks; the residues are shown in green sticks except for Glu124 that is shown in yellow. The insert figure shows the closest distance between the fluorine of quinazolinone derivative **28** and phenyl ring in Phe279 on the receptor. Adapted with permission from ref. <sup>96</sup> Copyright 2018 American Chemical Society.

initially reported by Bayer (**19**) as their starting point for SAR studies. The study identified 3 small molecule derivatives with low nanomolar to sub-nanomolar binding affinities toward the receptor (Figure 16). One key structural modification was the replacement of the fluorophenyl group with a benzothiazolyl group, which resulted in improved binding affinities. Additionally, modifying the alkyl substituent on the piperidine nitrogen to a fluoroethyl group allowed incorporation of fluorine in a position readily accessible for radiosynthetic incorporation

of fluorine-18. Two derivatives bearing fluorine substituents, **26** and **27**, possessed low nanomolar affinity toward the receptor with  $\text{IC}_{50}$  values of 9.3 nM and 20.6 nM, respectively. Both compounds were successfully radiolabeled with fluoride-18 through nucleophilic aliphatic substitution of a tosylate precursor with fluoride-18 in radiochemical yields of 10.3% and 7.0% respectively. An additional fluorine-bearing derivative identified in this work, **28**, retained the isopropyl group off the piperidine nitrogen, but rather

**Table 2.** *In vitro* Properties and Radiosynthetic Results of Small Molecule GHSR Imaging Probes.

Compound No.	IC <sub>50</sub>	EC <sub>50</sub>	RCY	clogD	Imaging Modality	Ref.
<b>20</b> (fig. 12)	22 nM <sup>[a]</sup>	N.R.	25%	4.1	<sup>11</sup> C-PET	91
<b>21</b> (fig. 13)	16 nM <sup>[a]</sup>	N.R.	2.5%	5.4	<sup>18</sup> F-PET	92
<b>22</b> (fig. 13)	4.0 nM <sup>[a]</sup>	N.R.	1.7%	5.1	<sup>11</sup> C-PET	92
<b>23</b> (fig. 13)	7.0 nM <sup>[a]</sup>	N.R.	16%	3.9	<sup>11</sup> C-PET	92
<b>(S)-24</b> (fig. 15)	2.2 nM	0.7 nM	N.R.	2.1	<sup>18</sup> F-PET	94
<b>(R)-24</b> (fig. 15)	3.9 nM	0.6 nM	N.R.	2.1	<sup>18</sup> F-PET	94
<b>25</b> (fig. 15)	2.7 nM	1.0 nM	N.R.	2.9	<sup>18</sup> F-PET	94
<b>26</b> (fig. 16)	9.3 nM	N.R.	7.0%	4.25	<sup>18</sup> F-PET	96
<b>27</b> (fig. 16)	20.6 nM	N.R.	10.3%	3.40	<sup>18</sup> F-PET	96
<b>28</b> (fig. 16)	0.02 nM	N.R.	N.R.	2.39	<sup>18</sup> F-PET	96

N.R. – not reported.

<sup>[a]</sup> Reported as K<sub>i</sub>.

incorporated fluorine in place of the methyl group on the tolyl portion of the molecule. The resulting lead candidate showed sub-nanomolar binding affinity with an IC<sub>50</sub> of 0.02 nM, which represents the strongest binding affinity of any GHSR ligand reported to date. In order to better comprehend the binding mode of quinazolinone derivatives toward the GHSR, the authors performed molecular docking studies with several of their developed derivatives, including compound **28**, utilizing a previously validated homology model of the GHSR (Figure 17A).<sup>85</sup> The docked poses placed the piperidine amine in close proximity to Glu124 on the receptor, which is regarded as an anchoring point for binding via an ionic interaction. Significant  $\pi$ - $\pi$  stacking interactions between the aromatic substituents on the small molecules and Phe279 and Tyr106 in the receptor were established. Interestingly, the fluorine in compound **28** was involved in the  $\pi$ - $\pi$  stacking interaction with Phe279 resulting in an additional binding interaction, not observed in derivatives bearing the methylphenyl group, that may contribute to its unprecedented binding affinity (Figure 17B). Radiolabeling of **28** with fluoride-18 was attempted through nucleophilic aromatic substitution of a nitro-bearing precursor. However, the labeling attempts were unsuccessful possibly due to the insufficient activation of the aromatic ring. Further development of the radiosynthesis for this molecule has yet to be reported.

## Conclusions

Since the discovery of the GHSR, there has been a growing interest in advancing our understanding of this receptor's dynamic processes and exploring the therapeutic potential of pharmaceuticals for this target. Molecular imaging provides a minimally invasive window into investigating GHSR expression in normal and disease states. In the last decade, the number of molecular imaging agents targeting this receptor has steadily grown resulting in probes for nuclear imaging modalities (SPECT/PET) using <sup>11</sup>C, <sup>18</sup>F, <sup>68</sup>Ga and <sup>99m</sup>Tc radioisotopes, and optical imaging through fluorescent dyes. This development has resulted in novel ligands with high affinity for the GHSR based on ghrelin, growth hormone secretagogues, and small molecules previously discovered for therapeutic

applications. These probes continue to evolve as researchers seek to optimize their physical and biological properties and proceed to *in vivo* evaluation. The optical imaging probes have been used for cellular and tissue imaging to investigate the GHSR as a potential biomarker for cardiac disease, and PET imaging probes are being developed for potential cancer and brain imaging. In addition to the incorporation of imaging moieties onto known GHSR compounds, novel ligands with imaging in mind have resulted from structure-activity relationship studies. The acquisition of knowledge regarding the dynamic function of this receptor and ghrelin is continuing to unfold, revealing numerous therapeutic possibilities. The integration of GHSR targeted imaging probes with ligands currently under investigation as potential therapeutics could be a step toward a more harmonized approach in drug research providing valuable information on biodistribution, kinetics, and metabolic behavior of such drug molecules and the treatment monitoring of receptor-influenced disorders.

## Declaration of Conflicting Interests

The author(s) declared no potential conflicts of interest with respect to the research, authorship, and/or publication of this article.

## Funding

The author(s) disclosed receipt of the following financial support for the research, authorship, and/or publication of this article: We gratefully acknowledge the support of the Natural Sciences and Engineering Research Council of Canada (NSERC) and the Molecular Imaging Collaborative Program at the University of Western Ontario.

## ORCID iDs

Marina D. Childs  <https://orcid.org/0000-0003-4735-8360>

Leonard G. Luyt  <https://orcid.org/0000-0002-0941-4731>

## References

- Howard AD, Feighner SD, Cully DF, et al. A receptor in pituitary and hypothalamus that functions in growth hormone release. *Science*. 1996;273(5277):974–9717.
- Bowers CY, Momany FA, Reynolds GA, Hong A. On the *in vitro* and *in vivo* activity of a new synthetic hexapeptide that acts on the

- pituitary to specifically release growth hormone. *Endocrinology*. 1984;114(5):1537–1545.
3. Bowers CY. GH releasing peptides – structure and kinetics. *J Pediatr Endocrinol Metab*. 1993;6(1):21–31.
  4. Deghenghi R, Cananzi MM, Torsello A, Battisti C, Muller EE, Locatelli V. GH-releasing activity of hexarelin, a new growth hormone releasing peptide, in infant and adult rats. *Life Sci*. 1994;54(18):1321–1328.
  5. Patchett AA, Nargund RP, Tata JR, et al. Design and biological activities of L-163,191 (MK-0677): a potent, orally active growth hormone secretagogue. *Proc Natl Acad Sci U S A*. 1995;92(15):7001–7005.
  6. Elias KA, Ingle GS, Burnier JP, et al. In vitro characterization of four novel classes of growth hormone-releasing peptide. *Endocrinology*. 1995;136(12):5694–5699.
  7. Raun K, Hansen BS, Johansen NL, et al. Ipamorelin, the first selective growth hormone secretagogue. *Eur J Endocrinol*. 1998;139(5):552–561.
  8. Moulin A, Ryan J, Martinez J, Fehrentz JA. Recent developments in ghrelin receptor ligands. *ChemMedChem*. 2007;2(9):1242–1259.
  9. Ueberberg B, Unger N, Saeger W, Mann K, Petersenn S. Expression of ghrelin and its receptor in human tissues. *Horm Metab Res*. 2009;41(1):814–821.
  10. Gnanapavan S, Kola B, Bustin S, et al. The tissue distribution of mRNA of ghrelin and subtypes of its receptor, GHS-R, in humans. *J Clin Endocrinol Metab*. 2002;87(6):2988–2991.
  11. Kojima M, Hosoda H, Date Y, Nakazato M, Matsuo H, Kangawa K. Ghrelin is a growth-hormone-releasing acylated peptide from stomach. *Nature*. 1999;402(6762):656–660.
  12. Zhu X, Cao Y, Voodg K, Steiner DF. On the processing of proghrelin to ghrelin. *J Biol Chem*. 2006;281(50):38867–38870.
  13. Yang J, Brown MS, Liang G, Grishin NV, Goldstein JL. Identification of the acyltransferase that octanoylates ghrelin, an appetite-stimulating peptide hormone. *Cell*. 2008;132(3):387–396.
  14. Gutierrez JA, Solenberg PJ, Perkins DR, et al. Ghrelin octanoylation mediated by an orphan lipid transferase. *Proc Natl Acad Sci U S A*. 2008;105(17):6320–6325.
  15. Lim CT, Kola B, Grossman A, Korbonits M. The expression of ghrelin O-acyltransferase (GOAT) in human tissues. *Endocr J*. 2011;58(8):707–710.
  16. Bednarek MA, Feighner SD, Pong SS, et al. Structure – Function studies on the new growth hormone-releasing peptide, ghrelin: Minimal sequence of ghrelin necessary for activation of growth hormone secretagogue receptor 1a. *J Med Chem*. 2000;43(23):4370–4376.
  17. Chen CY, Inui A, Asakawa A, et al. Des-acyl ghrelin acts by CRF type 2 receptors to disrupt fasted stomach motility in conscious rats. *Gastroenterology*. 2005;129(1):8–25.
  18. Zanetti M, Cappellari GG, Graziani A, Barazzoni R. Unacylated ghrelin improves vascular dysfunction and attenuates atherosclerosis during high-fat diet consumption in rodents. *Int J Mol Sci*. 2019;20(3):499.
  19. Huynh DN, Elimam H, Bessi VL, et al. A linear fragment of unacylated ghrelin (UAG 6–13) protects against myocardial ischemia/reperfusion injury in mice in a growth hormone secretagogue receptor-independent manner. *Front Endocrinol (Lausanne)*. 2019;9:798.
  20. Allas S, Caixàs A, Poitou C, et al. AZP-531, an unacylated ghrelin analog, improves food-related behavior in patients with Prader-Willi syndrome: A randomized placebo-controlled trial. *PLoS One*. 2018;13(1):e0190849.
  21. Yin Y, Li Y, Zhang W. The growth hormone secretagogue receptor: its intracellular signaling and regulation. *Int J Mol Sci*. 2014;15(3):4837–4855.
  22. Chow KBS, Sun J, Man Chu K, Tai Cheung W, Cheng CHK, Wise H. The truncated ghrelin receptor polypeptide (GHS-R1b) is localized in the endoplasmic reticulum where it forms heterodimers with ghrelin receptors (GHS-R1a) to attenuate their cell surface expression. *Mol Cell Endocrinol*. 2012;348(1):247–254.
  23. Mear Y, Enjalbert A, Thirion S. GHS-R1a constitutive activity and its physiological relevance. *Front Neurosci*. 2013;7:87.
  24. Holst B, Cygankiewicz A, Jensen TH, Ankersen M, Schwartz TW. High constitutive signaling of the ghrelin receptor – identification of a potent inverse agonist. *Mol Endocrinol*. 2003;17(11):2201–2210.
  25. Ge X, Yang H, Bednarek MA, et al. LEAP2 is an endogenous antagonist of the ghrelin receptor. *Cell Metab*. 2018;27(2):461–469.e6.
  26. Krause A, Sillard R, Kleemeier B, et al. Isolation and biochemical characterization of LEAP-2, a novel blood peptide expressed in the liver. *Protein Sci*. 2003;12(1):143–152.
  27. Wang JH, Li HZ, Shao XX, et al. Identifying the binding mechanism of LEAP2 to receptor GHSR1a. *FEBS J*. 2019;286(7):1332–1345.
  28. M’Kadmi C, Cabral A, Barrile F, et al. N-Terminal Liver-Expressed Antimicrobial Peptide 2 (LEAP2) region exhibits inverse agonist activity toward the ghrelin receptor. *J Med Chem*. 2019;62(2):965–973.
  29. Lv Y, Liang T, Wang G, Li Z. Ghrelin, a gastrointestinal hormone, regulates energy balance and lipid metabolism. *Biosci Rep*. 2018;38(5):BSR20181061.
  30. Mihalache L, Gherasim A, Niț O, et al. Effects of ghrelin in energy balance and body weight homeostasis. *Hormones*. 2016;15(2):186–196.
  31. Kurowska P, Mlyczynska E, Rak A. Effect of ghrelin on the apoptosis of various cells. A critical review. *J Physiol Pharmacol*. 2019;70(1):3–13.
  32. Mao Y, Tokudome T, Kishimoto I. Ghrelin and blood pressure regulation. *Curr Hypertens Rep*. 2016;18(2):15.
  33. Tokudome T, Otani K, Miyazato M, Kangawa K. Ghrelin and the heart. *Peptides*. 2019;111:42–46.
  34. Chen W, Enriori PJ. Ghrelin: a journey from GH secretagogue to regulator of metabolism. *Transl Gastrointest Cancer*. 2015;4(1):14–27.
  35. Colldén G, Tschöp MH, Müller TD. Therapeutic potential of targeting the ghrelin pathway. *Int J Mol Sci*. 2017;18(4):798.
  36. da Silva Pereira JA, da Silva FC, de Moraes-Vieira PMM. The impact of ghrelin in metabolic diseases: an immune perspective. *J Diabetes Res*. 2017;2017:4527980.

37. Soares JB, Roncon-Albuquerque R, Leite-Moreira A. Ghrelin and ghrelin receptor inhibitors: agents in the treatment of obesity. *Expert Opin Ther Targets*. 2008;12(9):1177–1189.
38. Costantino L, Barlocco D. Ghrelin receptor modulators: a patent review (2011-2014). *Expert Opin Ther Pat*. 2014;24(9):1007–1019.
39. Cameron KO, Bhattacharya SK, Loomis AK. Small molecule ghrelin receptor inverse agonists and antagonists. *J Med Chem*. 2014;57(21):8671–8691.
40. Vodnik M, Štrukelj B, Lunder M. Ghrelin receptor ligands reaching clinical trials: from peptides to peptidomimetics; from agonists to antagonists. *Horm Metab Res*. 2016;48(1):1–15.
41. Beiras-Fernandez A, Kreth S, Weis F, et al. Altered myocardial expression of ghrelin and its receptor (GHSR-1a) in patients with severe heart failure. *Peptides*. 2010;31(12):2222–2228.
42. Lin TC, Hsiao M. Ghrelin and cancer progression. *Biochim Biophys Acta*. 2017;1868(1):51–57.
43. Wang W, Chen ZX, Guo DY, Tao YX. Regulation of prostate cancer by hormone-responsive G protein-coupled receptors. *Pharmacol Ther*. 2018;191:135–147.
44. Grönberg M, Nilsson C, Markholm I, et al. Ghrelin expression is associated with a favorable outcome in male breast cancer. *Sci Rep*. 2018;8(1):13586.
45. Chopin LK, Seim I, Walpole CM, Herington AC. The Ghrelin axis—does it have an appetite for cancer progression? *Endocr Rev*. 2012;33(6):849–891.
46. Nikolopoulos D, Theocharis S, Kouraklis G. Ghrelin's role on gastrointestinal tract cancer. *Surg Oncol*. 2010;19(1):e2–e10.
47. Lu C, McFarland MS, Nesbitt RL, et al. Ghrelin receptor as a novel imaging target for prostatic neoplasms. *Prostate*. 2012;72(8):825–833.
48. Aleksova A, Beltrami AP, Bevilacqua E, et al. Ghrelin derangements in idiopathic dilated cardiomyopathy: impact of myocardial disease duration and left ventricular ejection fraction. *J Clin Med*. 2019;8(8):1152.
49. Machado JF, Silva RD, Melo R, Correia JDG. Less exploited GPCRs in precision medicine: targets for molecular imaging and theranostics. *Molecules*. 2018;24(1):49.
50. Iliopoulos-Tsoutsouvas C, Kulkarni RN, Makriyannis A, Nikas SP. Fluorescent probes for G-protein-coupled receptor drug discovery. *Expert Opin Drug Discov*. 2018;13(10):933–947.
51. Matsumoto M, Hosoda H, Kitajima Y, et al. Structure-activity relationship of ghrelin: pharmacological study of ghrelin peptides. *Biochem Biophys Res Commun*. 2001;287(1):142–146.
52. Van Craenenbroeck M, Gregoire F, De Neef P, Robberecht P, Perret J. Ala-scan of ghrelin (1-14): interaction with the recombinant human ghrelin receptor. *Peptides*. 2004;25(6):959–965.
53. Rosita D, Dewit MA, Luyt LG. Fluorine and rhenium substituted ghrelin analogues as potential imaging probes for the growth hormone secretagogue receptor. *J Med Chem*. 2009;52(8):2196–2203.
54. Tornesello AL, Buonaguro L, Tornesello ML, Buonaguro FM. Recent developments in metal-based drugs and chelating agents for neurodegenerative diseases treatments. *Molecules* 2017;22(8):1282.
55. Boschi A, Uccelli L, Martini P. A picture of modern Tc-99 m radiopharmaceuticals: Production, chemistry, and applications in molecular imaging. *Appl Sci*. 2019;9(12):2526.
56. Lipiński PFJ, Garnuszek P, Maurin M, et al. Structural studies on radiopharmaceutical DOTA-minigastrin analogue (CP04) complexes and their interaction with CCK2 receptor. *EJNMMI Res*. 2018;8(1):33.
57. Chollet C, Bergmann R, Pietzsch J, Beck-Sickinge AG. Design, evaluation, and comparison of ghrelin receptor agonists and inverse agonists as suitable radiotracers for PET imaging. *Bioconjug Chem*. 2012;23(4):771–784.
58. Charron CL, McFarland MS, Dhanvantari S, Luyt LG. Development of a [<sup>68</sup>Ga]-ghrelin analogue for PET imaging of the ghrelin receptor (GHSR-1a). *MedChemCommun*. 2018;9(10):1761–1767.
59. Koźmiński P, Gniazdowska E. Synthesis and in vitro/in vivo evaluation of novel mono- and trivalent technetium-99 m labeled ghrelin peptide complexes as potential diagnostic radiopharmaceuticals. *Nucl Med Biol*. 2015;42(1):28–37.
60. Enderle T, Graf M, Hertel C, Zoffmann SJ, Kitas EA. *Fluorescently Labeled Growth Hormone Secretagogue*. Patent 7173 109B2, USA, 2007.
61. Leyris JP, Roux T, Trinquet E, et al. Homogeneous time-resolved fluorescence-based assay to screen for ligands targeting the growth hormone secretagogue receptor type 1a. *Anal Biochem*. 2011;408(2):253–262.
62. Kern A, Albarran-Zeckler R, Walsh HE, Smith RG. Apo-ghrelin receptor forms heteromers with DRD2 in hypothalamic neurons and is essential for anorexigenic effects of DRD2 agonism. *Neuron*. 2012;73(2):317–332.
63. Schaeffer M, Langlet F, Lafont C, et al. Rapid sensing of circulating ghrelin by hypothalamic appetite-modifying neurons. *Proc Natl Acad Sci U S A*. 2013;110(4):1512–1517.
64. McGirr R, McFarland MS, McTavish J, Luyt LG, Dhanvantari S. Design and characterization of a fluorescent ghrelin analog for imaging the growth hormone secretagogue receptor 1a. *Regul Pept*. 2011;172(1-3):69–76.
65. Soto EJJ, Agosti F, Cabral A, et al. Constitutive and ghrelin-dependent GHSR1a activation impairs CaV2.1 and CaV2.2 currents in hypothalamic neurons. *J Gen Physiol*. 2015;146(3):205–219.
66. Cabral A, Portiansky E, Sánchez-Jaramillo E, Zigman JM, Perello M. Ghrelin activates hypophysiotropic corticotropin-releasing factor neurons independently of the arcuate nucleus. *Psychoneuroendocrinology*. 2016;67:27–39.
67. Berrout L, Isokawa M. Ghrelin upregulates the phosphorylation of the GluN2B subunit of the NMDA receptor by activating GHSR1a and Fyn in the rat hippocampus. *Brain Res*. 2018;1678:20–26.
68. Cornejo MP, Barrile F, De Francesco PN, Portiansky EL, Reynaldo M, Perello M. Ghrelin recruits specific subsets of dopamine and GABA neurons of different ventral tegmental area sub-nuclei. *Neuroscience*. 2018;392:107–120.
69. Cabral A, Fernandez G, Perello M. Analysis of brain nuclei accessible to ghrelin present in the cerebrospinal fluid. *Neuroscience*. 2013;253:406–415.

70. Cabral A, Valdivia S, Fernandez G, Reynaldo M, Perello M. Divergent neuronal circuitries underlying acute orexigenic effects of peripheral or central Ghrelin: critical role of brain accessibility. *J Neuroendocrinol.* 2014;26(8):542–554.
71. Fernandez G, Cabral A, Andreoli MF, et al. Evidence supporting a role for constitutive ghrelin receptor signaling in fasting-induced hyperphagia in male mice. *Endocrinology.* 2018;159(2):1021–1034.
72. Cornejo MP, De Francesco PN, García Romero G, et al. Ghrelin receptor signaling targets segregated clusters of neurons within the nucleus of the solitary tract. *Brain Struct Funct.* 2018;223(7):3133–3147.
73. Cabral A, Cornejo MP, Fernandez G, et al. Circulating ghrelin acts on GABA neurons of the area postrema and mediates gastric emptying in male mice. *Endocrinology.* 2017;158(5):1436–1449.
74. Uriarte M, De Francesco PN, Fernandez G, et al. Evidence supporting a role for the blood-cerebrospinal fluid barrier transporting circulating ghrelin into the brain. *Mol Neurobiol.* 2019;56(6):4120–4134.
75. Lufrano D, Trejo SA, Llovera RE, et al. Ghrelin binding to serum albumin and its biological impact. *Mol Cell Endocrinol.* 2016;436:130–140.
76. Schellekens H, De Francesco PN, Kandil D, et al. Ghrelin's orexigenic effect is modulated via a serotonin 2c receptor interaction. *ACS Chem Neurosci.* 2015;6(7):1186–1197.
77. Douglas GAF, McGirr R, Charlton CL, et al. Characterization of a far-red analog of ghrelin for imaging GHS-R in P19-derived cardiomyocytes. *Peptides.* 2014;54:81–88.
78. Sullivan R, McGirr R, Hu S, et al. Changes in the cardiac GHSR1a-Ghrelin system correlate with myocardial dysfunction in diabetic cardiomyopathy in mice. *J Endocr Soc.* 2018;2(2):178–189.
79. Sullivan R, Randhawa VK, Stokes A, et al. Dynamics of the ghrelin/growth hormone secretagogue receptor system in the human heart before and after cardiac transplantation. *J Endocr Soc.* 2019;3(4):748–762.
80. Lalonde T, Shepherd TG, Dhanvantari S, Luyt LG. Stapled ghrelin peptides as fluorescent imaging probes. *Pept Sci.* 2018;111(1):e24055.
81. Holst B, Lang M, Brandt E, et al. Ghrelin receptor inverse agonists: identification of an active peptide core and its interaction epitopes on the receptor. *Mol Pharmacol.* 2006;70(3):936–946.
82. Murrell E, Kovacs MS, Luyt LG. A compact and synthetically accessible fluorine-18 labelled cyclooctyne prosthetic group for labelling of biomolecules by copper-free click chemistry. *ChemMedChem.* 2018;13(16):1625–1628.
83. Charron CL, Hou J, McFarland MS, Dhanvantari S, Kovacs MS, Luyt LG. Structure-activity study of ghrelin(1-8) resulting in high affinity fluorine-bearing ligands for the ghrelin receptor. *J Med Chem.* 2017;60(17):7256–7266.
84. Zhao F, Darling JE, Gibbs RA, Houglund JL. A new class of ghrelin O-acyltransferase inhibitors incorporating triazole-linked lipid mimetic groups. *Bioorganic Med Chem Lett.* 2015;25(14):2800–2803.
85. Hou J, Charron CL, Fowkes MM, Luyt LG. Bridging computational modeling with amino acid replacements to investigate GHS-R1a-peptidomimetic recognition. *Eur J Med Chem.* 2016;123:822–833.
86. Fowkes MM, Lalonde T, Yu L, Dhanvantari S, Kovacs MS, Luyt LG. Peptidomimetic growth hormone secretagogue derivatives for positron emission tomography imaging of the ghrelin receptor. *Eur J Med Chem.* 2018;157:1500–1511.
87. Abbas A, Yu L, Lalonde T, et al. Development and characterization of an 18F-labeled ghrelin peptidomimetic for imaging the cardiac growth hormone secretagogue receptor. *Mol Imaging.* 2018;17:1536012118809587.
88. Lalonde T, Fowkes MM, Hou J, et al. Single amino acid replacement in G-7039 leads to a 70-fold increase in binding toward GHS-R1a. *ChemMedChem.* 2019;14(20):1762–1766.
89. Barrile F, M'Kadmi C, De Francesco PN, et al. Development of a novel fluorescent ligand of growth hormone secretagogue receptor based on the N-Terminal Leap2 region. *Mol Cell Endocrinol.* 2019;498:110573.
90. Rudolph J, Esler WP, O'Connor S, et al. Quinazolinone derivatives as orally available ghrelin receptor antagonists for the treatment of diabetes and obesity. *J Med Chem.* 2007;50(21):5202–5216.
91. Potter R, Horti AG, Ravert HT, et al. Synthesis and in vivo evaluation of (S)-6-(4-fluorophenoxy)-3-((1-[11C]methylpiperidin-3-yl)methyl)-2-o-tolylquinazolin-4(3H)-one, a potential PET tracer for growth hormone secretagogue receptor (GHSR). *Bioorganic Med Chem.* 2011;19(7):2368–2372.
92. Kawamura K, Fujinaga M, Shimoda Y, et al. Developing new PET tracers to image the growth hormone secretagogue receptor 1a (GHS-R1a). *Nucl Med Biol.* 2017;52:49–56.
93. Esler WP, Rudolph J, Claus TH, et al. Small-molecule Ghrelin receptor antagonists improve glucose tolerance, suppress appetite, and promote weight loss. *Endocrinology.* 2007;148(11):5175–5185.
94. Moldovan RP, Els-Heindl S, Worm DJ, et al. Development of fluorinated non-peptidic ghrelin receptor ligands for potential use in molecular imaging. *Int J Mol Sci.* 2017;18(4):768.
95. Hanrahan P, Bell J, Bottomley G, et al. Substituted azaquinazolines as modulators of GHSr-1a for the treatment of type II diabetes and obesity. *Bioorganic Med Chem Lett.* 2012;22(6):2271–2278.
96. Hou J, Kovacs MS, Dhanvantari S, Luyt LG. Development of candidates for positron emission tomography (PET) imaging of ghrelin receptor in disease: design, synthesis, and evaluation of fluorine-bearing quinazolinone derivatives. *J Med Chem.* 2018;61(3):1261–1275.